This information is current as of July 5, 2012.

Targeting Stat3 Induces Senescence in Tumor Cells and Elicits Prophylactic and Therapeutic Immune Responses against Breast Cancer Growth Mediated by NK Cells and CD4 $^{+}$ T Cells

Mercedes Tkach, Lorena Coria, Cinthia Rosemblit, Martín A. Rivas, Cecilia J. Proietti, María Celeste Díaz Flaqué, Wendy Beguelin, Isabel Frahm, Eduardo H. Charreau, Juliana Cassataro, Patricia V. Elizalde and Roxana Schillaci

J Immunol published online 29 June 2012
http://www.jimmunol.org/content/early/2012/06/29/jimmunol.1102538

Supplementary Material **http://www.jimmunol.org/content/suppl/2012/06/29/jimmunol.1102538.DC1.html**

Subscriptions Information about subscribing to *The Journal of Immunology* is online at: http://jimmunol.org/subscriptions

Permissions Submit copyright permission requests at: http://www.aai.org/ji/copyright.html

Email Alerts Receive free email-alerts when new articles cite this article. Sign up at: http://jimmunol.org/cgi/alerts/etoc

The Journal of Immunology is published twice each month by The American Association of Immunologists, Inc., 9650 Rockville Pike, Bethesda, MD 20814-3994.
Copyright © 2012 by The American Association of Immunologists, Inc. All rights reserved.
Print ISSN: 0022-1767 Online ISSN: 1550-6606.

Downloaded from http://jimmunol.org/ at UNIVERSIDAD DE BUENOS AIRES on July 5, 2012

Published June 29, 2012, doi:10.4049/jimmunol.1102538

Targeting Stat3 Induces Senescence in Tumor Cells and Elicits Prophylactic and Therapeutic Immune Responses against Breast Cancer Growth Mediated by NK Cells and CD4$^+$ T Cells

Mercedes Tkach,* Lorena Coria,† Cinthia Rosemblit,* Martín A. Rivas,*,[1] Cecilia J. Proietti,* María Celeste Díaz Flaqué,* Wendy Beguelin,* Isabel Frahm,‡ Eduardo H. Charreau,* Juliana Cassataro,† Patricia V. Elizalde,* and Roxana Schillaci*

Aberrant Stat3 activation and signaling contribute to malignant transformation by promoting cell cycle progression, inhibiting apoptosis, and mediating tumor immune evasion. Stat3 inhibition in tumor cells induces the expression of chemokines and proinflammatory cytokines, so we proposed to apply Stat3-inhibited breast cancer cells as a source of immunogens to induce an antitumor immune response. Studies were performed in two murine breast cancer models in which Stat3 is activated: progestin-dependent C4HD cells and 4T1 cells. We immunized BALB/c mice with irradiated cancer cells previously transfected with a dominant-negative Stat3 vector (Stat3Y705F) in either a prophylactic or a therapeutic manner. Prophylactic administration of breast cancer cells transfected with Stat3Y705F (Stat3Y705F-breast cancer cells) inhibited primary tumor growth compared with administration of empty vector-transfected cells in both models. In the 4T1 model, 50% of the challenged mice were tumor free, and the incidence of metastasis decreased by 90%. In vivo assays of C4HD tumors showed that the antitumor immune response involves the participation of CD4$^+$ T cells and cytotoxic NK cells. Therapeutic immunization with Stat3Y705F-breast cancer cells inhibited tumor growth, promoted tumor cell differentiation, and decreased metastasis. Furthermore, inhibition of Stat3 activation in breast cancer cells induced cellular senescence, contributing to their immunogenic phenotype. In this work, we provide preclinical proof of concept that ablating Stat3 signaling in breast cancer cells results in an effective immunotherapy against breast cancer growth and metastasis. Moreover, our findings showing that Stat3 inactivation results in induction of a cellular senescence program disclose a potential mechanism for immunotherapy research. ***The Journal of Immunology*****, 2012, 189: 000–000.**

Stat3 controls genes are involved in cell proliferation and in the production of angiogenic and antiapoptotic factors (1, 2). Moreover, Stat3 has recently been shown to mediate tumor-induced immunosuppression at many levels (3, 4). Stat3 activation in tumor cells not only inhibits the production of immunostimulatory mediators but also promotes the secretion of immunosuppressive factors that, in turn, activate Stat3 in tumor-interacting cells (5). This feed-forward mechanism leads to tumor immune evasion through the suppression of innate and adaptive antitumor immune responses (6).

Numerous studies have reported persistent activation of Stat3 in a wide variety of human tumors (7); in particular, Stat3 plays a key role in mammary cancer by promoting breast tumorigenesis (8) and conferring resistance to apoptosis (9). Stat3 is also associated with breast cancer chemotherapeutic resistance (10). Taken together, these findings highlight Stat3 as an interesting molecular target for breast cancer immunotherapy.

Current immunotherapy protocols are based on immunization with one of the few characterized cancer Ags or with whole cancer cells that have been engineered to modify the expression of cytokines and/or costimulatory molecules and thereby render them immunogenic. Even with these protocols, the addition of adjuvants is sometimes necessary to promote nonspecific inflammation. We hypothesized that blocking Stat3 in breast cancer cells would result in a useful cell-based immunogen capable of activating innate and adaptive antitumor immune responses. Thus, we designed an

*Laboratorio de Mecanismos Moleculares de Carcinogénesis, Instituto de Biología y Medicina Experimental, Consejo Nacional de Investigaciones Científicas y Técnicas de Argentina, C1428ADN Buenos Aires, Argentina; †Laboratorio de Inmunogenética, Hospital de Clínicas, Facultad de Medicina, Universidad de Buenos Aires, Buenos Aires, Argentina; and ‡Servicio de Patología, Sanatorio Mater Dei, Buenos Aires, Argentina

[1]Current address: Experimental Therapeutics Laboratory, Vall d'Hebron Institute of Oncology, Barcelona, Spain.

Received for publication September 7, 2011. Accepted for publication May 21, 2012.

This work was supported by Susan G. Komen for the Cure Investigator-Initiated Research Grant KG090250, National Agency of Scientific Promotion of Argentina Grants IDB/PICT 2010-211 and Argentina National Council of Scientific Research Grant PIP 737, Fundación A. Roemmers and Oncomed-Reno Consejo Nacional de Investigaciones Científicas y Técnicas de Argentina Grant 1819/03 from the Henry Moore Institute of Argentina.

Address correspondence and reprint requests to Dr. Roxana Schillaci, Laboratorio de Mecanismos Moleculares de Carcinogénesis, Instituto de Biología y Medicina Experimental, Consejo Nacional de Investigaciones Científicas y Técnicas de Argentina, Vuelta de Obligado 2490, C1428ADN Buenos Aires, Argentina. E-mail address: rschillaci@ibyme.conicet.gov.ar

The online version of this article contains supplemental material.

Abbreviations used in this article: DC, dendritic cell; DN, dominant-negative; DTH, delayed-type hypersensitivity assay; β-gal, β-galactosidase; MPA, medroxyprogesterone acetate; pcDNA3.1-C4HD, C4HD cell transfected with pcDNA3.1 vector; pcDNA3.1-4T1, 4T1 cell transfected with pcDNA3.1 vector; RAE-1, retinoic acid early inducible-1; SA-β-Gal, senescence-associated acidic β-galactosidase; Stat3Y705F-C4HD, C4HD cell transfected with Stat3 dominant-negative vector, Stat3Y705F; Stat3Y705F-4T1, 4T1 cell transfected with Stat3 dominant-negative vector, Stat3Y705F; Treg, tumor-infiltrating regulatory T cell.

Copyright © 2012 by The American Association of Immunologists, Inc. 0022-1767/12/$16.00

Downloaded from http://jimmunol.org/ at UNIVERSIDAD DE BUENOS AIRES on July 5, 2012

immunotherapy approach based on serial inoculation of murine breast cancer cells transfected with the dominant-negative (DN) Stat3 expression vector Stat3Y705F. Our results showed that this immunization protocol inhibited wild-type tumor growth in vivo in BALB/c mice through the activation of cellular immune responses involving $CD4^+$ T cells and cytotoxic NK cells. Immunization with Stat3Y705F-breast cancer cells developed an antitumor immune memory able to inhibit not only parental tumor growth but also other syngeneic mammary tumor and non-organ–related tumor. Interestingly, this immunotherapy also overcame the immune tolerance induced by tumor cells to decrease the growth of an established breast cancer and to prevent metastasis.

It has been shown that oncogene inactivation induces cellular senescence and the secretion of proinflammatory cytokines in diverse tumor types (11, 12). Because Stat3 is a signaling node for multiple oncogenic pathways, we wondered whether Stat3 inhibition was associated with cellular senescence. Interestingly, we observed that inhibition of Stat3 was associated with upregulation of senescence markers such as acidic β-galactosidase (β-gal) staining, induction of p16INK4a and p15INK4b expression, and changes in chromatin structure such as increased methylation of histone H3. To our knowledge, these findings provide the first evidence that inhibition of Stat3 activation induces a cellular senescence program, likely creating a completely different tumor microenvironment. By blocking Stat3 activation in tumor cells, we have developed an effective whole-cell vaccine capable of inducing an antitumor immune response leading to the inhibition of tumor growth and metastasis.

Materials and Methods

Animals and tumors

Experiments were carried out in virgin female BALB/c mice, raised at the Institute of Biology and Experimental Medicine of Buenos Aires or in NIH (S)-nude mice obtained from National University of La Plata (Buenos Aires, Argentina), and were maintained in pathogen-free conditions. All animal studies were conducted as previously described (13), in accordance with the highest standards of animal care as outlined by the National Institutes of Health's *Guide for the Care and Use of Laboratory Animals* (14), and were approved by the Institute of Biology and Experimental Medicine Animal Research Committee. Hormone-dependent ductal tumor line C4HD was originated in mice treated with 40 mg medroxyprogesterone acetate (MPA; Gador, Buenos Aires, Argentina) every 3 mo for 1 y and were maintained by serial transplantation in animals treated with 40 mg s.c. depot–MPA in the opposite flank to tumor inoculum (15).

Cell culture

Primary cultures of epithelial cells from C4HD tumors growing in MPA-treated mice were performed as described previously (13, 16, 17). C4HD cells are sensitive to progestin; all the experiments were performed in DMEM/F12 without phenol red (Sigma-Aldrich, St. Louis, MO) plus 2.5% charcoal-stripped FCS supplemented with 10 nM MPA (Sigma-Aldrich). 4T1 mouse mammary tumor cells, CT26 mouse colon carcinoma, and YAC-1 cell line were obtained from the American Type Culture Collection (Manassas, VA), cultured in RPMI 1640 medium (Life Technologies, Grand Island, NY), and supplemented with 10% FCS (Gen, Buenos Aires, Argentina). In some experiments, 2 μM JSI-124 (Calbiochem, Gibbstown, NJ) was used.

Tumor experiments

Cell transfection and immunization protocol. C4HD and 4T1 cells plated in 100-mm dishes were transiently transfected for 48 h with 11 μg of the DN Stat3 expression vector, Stat3Y705F (18, 19) with FugeneHD transfection reagent (Roche Biochemicals, Indianapolis, IN). C4HD and 4T1 cells were then inactivated by irradiation with 50 or 100 Gy ^{60}Co, respectively. Mice (BALB/c or nude, $n = 5$) were injected s.c. in the right flank with 2×10^6 irradiated Stat3Y705F-transfected C4HD or 4T1 cells at 6, 4, and 2 wk prior to challenge with a fragment of C4HD tumor or with 1×10^4 4T1 cells implanted into the fourth mammary gland or with 4×10^5 CT26 cells. Simultaneously to C4HD tumor challenge, mice were inoculated with depot–MPA. Control groups included mice injected with PBS, with 2×10^6 cells or with 2×10^6 cells transfected with empty pcDNA3.1 vector and then irradiated. Animals were monitored, and tumor growth was measured three times a week as described previously (13).

Evaluation of pulmonary metastasis. BALB/c mice ($n = 8$) bearing 4T1 tumors were sacrificed, lungs were fixed with Bouin, and the number of superficial lung colonies was counted by an investigator who was blind to the experimental arm.

In vivo lymphocyte subset depletion. Immunized animals were depleted of $CD4^+$ and $CD8^+$ lymphocytes by i.p. administration of 0.5 mg mAbs/mouse against CD4 (clone YTS 191.1), CD8 (clone YTS 169.4), both from American Type Culture Collection, at days −1, 0, 1, 8, 15, and 22, relative to tumor inoculation (day 0). For NK cell depletion, mice were injected with 0.25 mg anti–asialo-GM1 Abs/mouse (Wako, Richmond, VA) on days −1, 7, 14, and 21. Control mice received equivalent amounts of normal rat or rabbit IgG at the same days. Depletions were confirmed in peripheral blood cells 7 d after tumor challenge by flow cytometry using non-cross–reactive Abs.

Delayed-type hypersensitivity assay. Delayed-type hypersensitivity assay (DTH) response was performed 1 wk after the last immunization injecting 3×10^5 cells in the left footpad and PBS in the right footpad as described previously (20).

Therapeutic immunization. In C4HD model, mice ($n = 5$) were challenged with a fragment of C4HD tumor and inoculated with depot–MPA and immunized with 2×10^6 irradiated C4HD cells transfected with Stat3 DN vector, Stat3Y705F (Stat3Y705F-C4HD) cells or control cells by s.c. injection on days 6 and 18. In the 4T1 model, mice ($n = 5$) were inoculated with 1×10^4 cells by s.c. injection and immunized with 1×10^6 irradiated 4T1 cells transfected with Stat3 DN vector, Stat3Y705F (Stat3Y705F-4T1) cells on days 4, 11, and 18.

Cytokine production

Mitomycin C-inactivated C4HD cells (8×10^4/ml) were cocultured with splenocytes (4×10^6/ml) isolated from immunized animals for 48 h. Evaluation of cytokine production (IFN-γ, IL-2, IL-10, and IL-4) was quantified by sandwich ELISA using paired cytokine-specific mAbs according to the manufacturer's instructions (BD Pharmingen, San Diego, CA).

For intracellular IFN-γ detection, splenocytes (2×10^6 cells/ml) were plated in complete RPMI 1640 medium with 10 U/ml human rIL-2 (PeproTech, Rocky Hill, NJ) in the presence or absence of mitomycin C-treated C4HD cells for 18 h or in the presence of 1 ng/ml IL-12 (PeproTech). Monensin (10 μg/ml; Sigma-Aldrich) was added to the cells for the last 4 h of culture. Cells were stained with different combinations of fluorochrome-coupled Abs against CD4 (FITC), CD3 (PE), and DX5 (allophycocyanin) (eBioscience, San Diego, CA). To determine IFN-γ production, cells were additionally labeled with anti–IFN-γ (PercpCy5.5) (eBioscience) after treatment with a Fixation and Permeabilization kit (eBioscience), according to the manufacturer's instructions. Isotype-matched Abs were incubated in parallel with all experimental samples. Flow cytometry acquisition was done on a FACSAria (BD Biosciences, San Jose, CA) and analyzed using FlowJo software (Tree Star).

Cytokine Ab arrays for detecting cultured C4HD cytokine secretion after Stat3 activation blockage were developed according to the manufacturer's protocol (Panomics, Redwood City, CA).

Evaluation of tumor-infiltrating lymphocytes

4T1 or C4HD primary tumors were removed from mice ($n = 5$) and digested in 400 U/ml collagenase type II (Invitrogen Life Technologies, Carlsbad, CA) and 50 U/ml DNase I (Thermo Scientific, Pittsburgh, PA) solution for 1 h at 37°C. Cells were incubated for 30 min with CD16/32 (Fc block; eBioscience), and tumor-infiltrating cells were directly stained with conjugated Abs for phenotype characterization by flow cytometry. The following Abs were used: CD45 (allophycocyanin), CD3 (FITC or PeCy5), DX5 (allophycocyanin), CD4 (FITC), CD8 (PE), Foxp3 (PE), and CD25 (allophycocyanin) (eBioscience).

CD69 expression and IFN-γ production in $CD4^+$ T and NK cells were determined in infiltrating cell suspensions stimulated with 10 ng/ml PMA for 5 h. Monensin was added together with the stimuli, and at the end of the culture, IFN-γ was measured by intracellular flow cytometry as described above. Membrane expression of CD69 was performed by direct immunofluorescence using anti-CD69 (PE) Ab (eBioscience), followed by flow cytometry analysis.

NK cells isolation, cytotoxicity, and degranulation assay

Splenocytes or NK cell-mediated cytotoxicity was analyzed by a standard [^{51}Cr] release assay as described previously (20). Briefly, target C4HD or YAC-1

Downloaded from http://jimmunol.org/ at UNIVERSIDAD DE BUENOS AIRES on July 5, 2012

(1×10^4 cells), labeled with 100 uCi $Na_2{}^{51}CrO_4$ (NEN, Waltham, MA), were mixed with splenocytes previously cocultured for 5 d with wild-type mitomycin C-treated C4HD cells at different ratios for 4 h. In the case of in vitro effector lymphocyte subset depletion, splenocytes were depleted of $CD4^+$ or $CD8^+$ cells using Dynabeads Mouse CD4 (L3T4) or Mouse CD8 (L3T8), respectively (Dynal Biotech, Invitrogen) or of NK cells using EasySep Mouse panNK (CD49b) Positive Selection Kit (StemCell Technologies, Vancouver, BC, Canada), according to the manufacturer's instructions. In the case of NK cell cytotoxicity assay, NK cells were purified by negative selection using the Mouse NK Cell Enrichment Set-DM (BD Biosciences). Then, C4HD or YAC-1 target cells labeled with [^{51}Cr] were added. After incubation, radioactivity released was counted in a gamma counter. The percentage of specific lysis was calculated as follows: percent-specific lysis = [(experimental cpm − spontaneous cpm)/(maximal cpm − spontaneous cpm)].

For degranulation evaluation, splenocytes were cultured alone or with mitomycin C-treated C4HD overnight at 37°C. During the last 4 h, CD107a mAb was added. Cells were harvested and stained with CD3 and DX5 Abs to gate NK cells ($CD3^-DX5^+$ cells) and to determine the percentage of $CD107a^+$ cells by flow cytometry.

β-Gal activity at pH 6

Cells were washed twice in PBS, fixed in 3% formaldehyde, and washed again in PBS. The cells were incubated overnight at 37°C (without CO_2) with freshly prepared β-gal staining solution (21).

Splenocyte proliferation assay

Two weeks after last immunization, splenocytes were isolated and plated into 96-well plate, and its proliferation was performed by [^{3}H]thymidine incorporation assay by quadruplicate as described previously (20).

Activation of splenic dendritic cells

In vitro induction of dendritic cells (DCs) activation was evaluated by measuring the expression of various surface markers by flow cytometry. Splenocytes from immunized animals were cocultured with mitomycin C-treated C4HD cells for 48 h and then stained with conjugated Abs specific for CD11c (FITC), CD40 (allophycocyanin), CD86 (PE), and MHC class II (PeCy5) or isotype control (eBioscience). After staining, cells were fixed and analyzed by flow cytometry, using a FACSAria (BD Biosciences). Data were analyzed using FlowJo software (Tree Star).

For ex vivo analysis of DC activation, cell suspensions were obtained from draining lymph nodes, and spleens were stained as described above.

Expression of retinoic acid early inducible-1 and H-60

C4HD cells growing in 10 nM MPA were harvested and stained with anti-mouse H-60–PE and anti-mouse retinoic acid early inducible-1 (RAE-1)–allophycocyanin or with the corresponding isotype control (R&D Systems) and analyzed by flow cytometry.

Western blot analysis

Protein extracts were analyzed by Western blot performed as previously described (20) using the following Abs: phospho-Stat3 (Tyr^{705}) (B-7), total Stat3 (C-20), p16INK4a (M-156), and p15INK4b (K-18) all from Santa Cruz Biotechnology (Santa Cruz, CA); FLAG-M2 mAb from Sigma-Aldrich; and trimethyl K9 histone H3 from Millipore (Billerica, MA).

Histopathological analysis

Tumors were excised and fixed in 10% buffered formalin. Representative fragments were embedded in paraffin, and 5-μm sections were obtained and stained with H&E for microscopic observations.

Immunofluorescence detection of trimethyl K9 histone H3

Transfected cells grown on glass coverslips were fixed and permeabilized in ice-cold methanol and were then blocked with PBS–1% BSA. Trimethyl K9 histone H3 was detected using a rabbit mAb (Millipore), followed by incubation with a goat anti-rabbit IgG–Alexa 488 (Molecular Probes, Eugene, OR) secondary Ab. Cells were analyzed by using a Nikon Eclipse E800 confocal laser microscopy system.

Statistical analysis

The differences between control and experimental groups were analyzed by ANOVA, followed by Tukey *t* test between groups. Linear regression analysis was performed on tumor growth curves, and the slopes were compared using ANOVA, followed by a parallelism test to evaluate the statistical significance of the differences. A p value < 0.05 was accepted as statistically significant. Comparison of the number of lung metastasis among different groups was done by the nonparametric Mann–Whitney *U* test. Kaplan–Meier curves were generated by using GraphPad Prism software and analyzed with log-rank test.

Results

Inhibition of Stat3 induces cellular senescence and secretion of proinflammatory cytokines and chemokines in breast cancer cells

In this study, we used primary cultures of epithelial cells from the progestin-dependent C4HD tumor and the murine cell line 4T1. In a previous study, we demonstrated that progestins induce Stat3 activation in C4HD cells and that the presence of activated Stat3 is required for progestin stimulation of breast cancer growth (19). The 4T1 cell line, which is derived from a BALB/c mouse mammary carcinoma (22, 23), displays constitutive activation of Stat3 (24). Tumors derived from this cell line are widely used in immunotherapy studies. These tumors resemble stage IV human mammary cancers and have a high incidence of lung and liver metastasis (22, 23). In addition, both C4HD cells and 4T1 cells are poorly immunogenic (20, 22, 23).

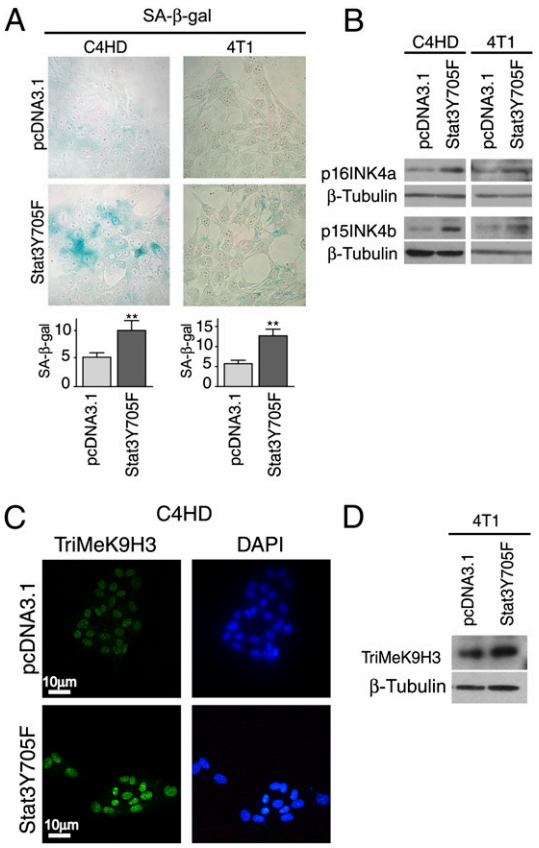

FIGURE 1. Inhibition of Stat3 activation induces expression of cellular senescence markers and changes in chromatin structure in vitro. (**A**) SA-β-gal staining was performed in C4HD and 4T1 cell lines transfected with pcDNA3.1 or Stat3Y705F. Data are presented as the means ± SE of the percentages of SA-β-gal–positive cells. Original magnification ×400. $^{**}p < 0.01$. (**B**) Cell lysates of C4HD and 4T1 cells transfected with pcDNA3.1 or Stat3Y705F were analyzed by Western blotting for p16INK4a and p15INKb expression. (**C**) Immunofluorescence staining with anti–trimethyl-K9 histone H3 Ab upon pcDNA3.1 or Stat3Y705F transfection of C4HD cells by confocal microscopy. (**D**) Western blots for pcDNA3.1-transfected and Stat3Y705F-transfected 4T1 cells probed with Abs specific for trimethyl-K9 histone H3 and β-tubulin.

Downloaded from http://jimmunol.org/ at UNIVERSIDAD DE BUENOS AIRES on July 5, 2012

Stat3 signaling in cancer cells negatively regulates the cells' ability to express inflammatory mediators. To study whether inhibition of Stat3 activation in C4HD cells could alter this tumor phenotype, we transfected C4HD cells cultured in 10 nM MPA with the Stat3Y705F expression vector to generate Stat3Y705F-C4HD cells or treated C4HD cells with 2 μM JSI-124, a pharmacological inhibitor of Stat3 phosphorylation (25) (Supplemental Fig. 1A). We then detected changes in cytokine and chemokine secretion using an Ab array. Similar to previous results for B16, SCK, and CT26 cells (6), inhibition of Stat3 activation in C4HD cells resulted in a strong upregulation of proinflammatory cytokines, including IL-6, IL-5, TNF-α, and IFN-γ, and chemokines, including IFN-γ–inducible protein-10 (IP-10) and RANTES (Supplemental Fig. 1B, 1C).

Cellular senescence is an important mechanism of tumor regression upon oncogene inactivation (11), and this process leads to the secretion of proinflammatory cytokines (12); therefore, we wondered whether in addition to inducing apoptosis (9, 19), Stat3 inhibition could also drive a senescence program. To address this question, we performed several senescence assays in tumor cells transfected with Stat3Y705F. Suppression of Stat3 activation in C4HD and 4T1 cells resulted in senescence-associated acidic β-gal (SA-β-Gal) staining (Fig. 1A) and increased expression of the senescence-associated markers p15INK4b and p16INK4a (Fig. 1B). Cellular senescence is also associated with global changes in chromatin structure such as histone methylation. We observed that Stat3Y705F-C4HD and Stat3Y705F-4T1 cells showed a marked increase in trimethyl-K4 histone H3 (Fig. 1C, 1D, respectively) when compared with control cells. These findings suggest that breast cancer cells undergo senescence and secrete proinflammatory cytokines and chemokines upon Stat3 inhibition.

Immunization with tumor cells expressing a DN Stat3 protein induces an antitumor immune response

Because cytokines and chemokines are important for immune cell activation, cancer cell lines expressing a DN Stat3 protein provide

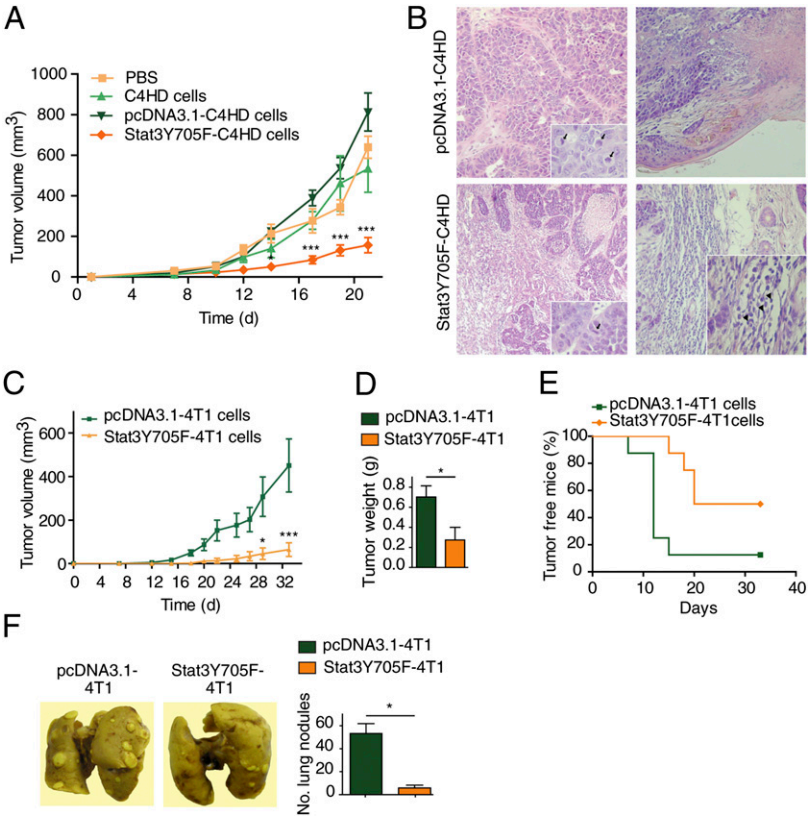

FIGURE 2. Induction of antitumor immunity against wild-type tumor growth in mice immunized with Stat3Y705-transfected C4HD cells or 4T1 cells. (**A**) BALB/c mice ($n = 5$) were injected s.c. with 2×10^6 irradiated Stat3Y705F- or pcDNA3.1-transfected C4HD cells or with wild-type C4HD cells or PBS 6, 4, and 2 wk prior to challenge with C4HD tumor cells. At the time of C4HD tumor challenge, mice were implanted with depot–MPA. ***$p < 0.001$. Similar results were obtained in four independent experiments. (**B**) Histopathological analysis of C4HD tumors. Tissue sections of C4HD tumors obtained from mice immunized with pcDNA3.1-C4HD cells (*upper panels*). Ductal mammary carcinoma composed of pseudolobules of highly cohesive glandular cells separated by scanty vascular stroma (H&E, original magnification ×100). Several mitotic figures are indicated by arrows in the higher magnification image (*inset*, H&E, original magnification, ×400). Tissue sections of C4HD tumors obtained from mice immunized with Stat3Y705F-C4HD cells (*lower panels*). The tumor shows necrosis, apoptosis, and hyalinization (*left panel*, H&E, original magnification ×100). In a nonnecrotic area, the tumor shows few mitotic figures (*inset*, H&E, original magnification ×400). These tumors display a high degree of lymphocyte infiltration (*right panel*, H&E, original magnification ×100), as indicated by the arrowhead in the *inset* (H&E, original magnification ×400) Mitotic count per high-power field, original magnification ×400, 10.5 ± 0.5 versus 3.8 ± 0.3; $p < 0.01$. (**C**) BALB/c mice were immunized with 4T1 cells transfected with Stat3Y705F or pcDNA3.1 as described above. Mice were then challenged with 1×10^4 4T1 cells. Each point represents the mean tumor volume of tumor-bearing mice (seven tumors ± SE of mice immunized with pcDNA3.1-4T1 cells versus four tumors ± SE of mice immunized with Stat3Y705F-4T1 cells). *$p < 0.05$, ***$p < 0.001$. (**D**) Tumor weight at the end of the experiment. *$p < 0.05$. (**E**) Percentage of tumor-free mice after 4T1 challenge of mice immunized with Stat3Y705F-4T1 or pcDNA3-4T1 cells. Data were evaluated using a Kaplan–Meier survival curve and log-rank test. $p < 0.01$. (**F**) Immunized mice were sacrificed, lungs were harvested and fixed, and the number of 4T1 tumor nodules was counted. Values represent mean numbers of colonies ± SE ($n = 8$). *$p < 0.05$. Representative photos of lungs excised from both groups are shown. Bouin staining, original magnification ×1.2. Similar results were obtained in three independent experiments. (A and C) Mice were assessed for the formation of tumors three times a week.

Downloaded from http://jimmunol.org/ at UNIVERSIDAD DE BUENOS AIRES on July 5, 2012

a potential immunogen able to induce an antitumor immune response. Thus, we designed an immunization protocol using Stat3Y705F-transfected cells and assessed the ability of this protocol to provide protection against wild-type tumor challenge. To this end, BALB/c mice were injected with Stat3Y705F-C4HD cells inactivated by irradiation 6, 4, and 2 wk before challenge with untransfected C4HD tumor cells. Mice were implanted with depot–MPA at the time of tumor challenge. As controls, mice were injected with PBS, C4HD cells treated with MPA (referred to as wild-type C4HD cells) or C4HD cells transfected with the empty pcDNA3.1 vector (referred to as pcDNA3.1-C4HD cells) treated with MPA and thereafter irradiated. On day 23, the mean volumes and growth rates of tumors that developed in mice injected with Stat3Y705F-C4HD cells were significantly lower than those of tumors from the control groups ($p < 0.001$; Fig. 2A, Table I). Histopathological analysis of C4HD tumors grown in mice injected with Stat3Y705F-C4HD cells showed extensive fibrotic and necrotic areas and lymphocyte infiltration (Fig. 2B). Moreover, these tumors also displayed a marked decrease in mitotic figures when compared with tumors from animals injected with pcDNA3.1-C4HD cells (Fig. 2B).

To test whether this immunization protocol is effective in other breast cancer models, we used the 4T1 mammary carcinoma cell line (22, 23). Immunization with irradiated 4T1 cells transfected in vitro with Stat3Y705F (Stat3Y705F-4T1 cells; Supplemental Fig. 1A) strongly inhibited wild-type 4T1 tumor growth ($p < 0.001$; Fig. 2C), decreased tumor weight ($p < 0.05$; Fig. 2D), and decreased the number of tumor-bearing mice ($p < 0.01$; Fig. 2E) compared with mice injected with pcDNA3.1-4T1 cells (Table I). Moreover, visible metastatic lesions and extensive dissemination were observed in the lungs of mice immunized with pcDNA3.1-4T1 cells, whereas a strong inhibition of lung metastasis was observed in Stat3Y705F-4T1–immunized animals ($p < 0.05$; Fig. 2F). Our findings indicate that immunization with Stat3Y705F-transfected breast cancer cells confers protection not only by decreasing tumor incidence and primary tumor growth but also by reducing the frequency of spontaneous lung metastasis.

$CD4^+$ T cells and NK cells are involved in the antitumor immune response elicited by Stat3Y705F–breast cancer cell immunization

Our results strongly suggested that immunization with Stat3Y705F-C4HD or Stat3Y705F-4T1 cells elicits a cellular immune response against parental tumor challenge in vivo. To confirm this, we assessed the DTH response. As shown in Fig. 3A, a marked increase in DTH reactivity was observed in mice injected with Stat3Y705F-C4HD cells when compared with control mice. To establish a requirement for T cells in the protective antitumor response in immunocompetent BALB/c mice, we repeated the immunization experiments following the exact experimental protocol described above in nude mice. Immunization of nude mice with Stat3Y705F-C4HD cells did not prevent C4HD tumor formation, and animals from all groups developed tumors at an equal rate (Fig. 3B). These results clearly show that T cells are involved in the antitumor effect observed in BALB/c mice immunized with Stat3Y705F-C4HD cells. To directly determine which immune cells mediate the antitumor effect observed, we performed in vivo experiments involving Ab-mediated depletion of $CD8^+$T cells, $CD4^+$ T cells, or NK cells before challenge with wild-type C4HD tumor cells. Flow cytometric analysis confirmed the depletion of the $CD3^+CD4^+$, $CD3^+CD8^+$, or NK ($CD3^-DX5^+$) cell populations (Supplemental Fig. 2). Depletion of $CD4^+$ T cells or NK cells abrogated the antitumor effect of Stat3Y705F-C4HD cell immunization, whereas depletion of $CD8^+$ T cells had no significant effect (Fig. 3C). Interestingly, we observed an increase in NK cells in the peripheral blood in Stat3Y705F-C4HD–immunized animals 1 wk after tumor challenge (Supplemental Fig. 2) and in draining lymph nodes after immunization (Fig. 3D). Because $CD4^+$ T cells were involved in the antitumor effect, we studied whether memory T cells were developed during the immunization protocol. Flow cytometry analysis showed that immunization with Stat3Y705F-C4HD cells significantly increased the $CD4^+CD44^+$ T cells memory population with respect to mice immunized with pcDNA3.1-C4HD cells (Fig. 3E). This increase was also observed in mice immunized with Stat3Y705F-4T1 cells when compared with control mice (data not shown). We observed an increase in the expression of CD86 and MHC class II in ex vivo DCs from spleen and lymph nodes of Stat3Y705F-C4HD–immunized animals when compared with the pcDNA3.1-C4HD cells group (Fig. 3F). Moreover, we also detected an augmentation in CD86 and MHC class II expression in DCs from spleen of Stat3Y705F-C4HD–immunized mice after coculture with C4HD cells (Fig. 3F). In ex vivo and in in vitro experiments, DCs showed no modification of CD40 expression (Fig. 3F). Next, we evaluated whether Stat3Y705F-4T1 cell immunization modulates the tumor milieu. Mice immunized with Stat3Y705F-4T1 cells displayed an

Table I. Prophylactic whole-cell vaccine

Protocol and Treatment	Mean Tumor Volume ± SEM (mm^3)	Mean Growth Rate ± SEM (mm^3/d)	% Growth Inhibition
C4HD immunization			
PBS	639.5 ± 54.3[a]	16.1 ± 1.8[a]	
Wild-type-C4HD	534.1 ± 116.6[a]	18.7 ± 3.7[a]	
pcDNA3.1-C4HD	662.6 ± 164.7[a]	21.4 ± 2.9[a]	
Stat3Y705F-C4HD	157.2 ± 37.3[b]	5.6 ± 1.4[b]	77.3,[c] 74.3,[d] and 78.2[e]
4T1 immunization			
pcDNA3.1-4T1	594.0 ± 259.0[a]	12.9 ± 1.8[a]	
Stat3Y705F-4T1	112.8 ± 79.8[b]	1.9 ± 0.5[b]	81.0[f]

Growth rates were calculated as the slopes of growth curves. Volume and percentage of growth inhibition in tumors from mice immunized with Stat3Y705F-C4HD cells with respect to mice immunized with control pcDNA3.1-C4HD cells or wild type-C4HD cells or injected with PBS were calculated at day 23. Volume and percentage of growth inhibition in tumors from mice immunized with Stat3Y705F-4T1 cells with respect to mice immunized with control pcDNA3.1-4T1 cells were calculated at day 33, as described in *Materials and Methods*.

[a]versus [b], $p < 0.001$.

[c]With respect to PBS, for growth inhibition, $p < 0.001$.

[d]With respect to wild type-C4HD cells, for growth inhibition, $p < 0.001$.

[e]With respect to pcDNA3.1-C4HD cells, for growth inhibition, $p < 0.001$.

[f]With respect to pcDNA3.1-4T1 cells, for growth inhibition, $p < 0.001$.

Downloaded from http://jimmunol.org/ at UNIVERSIDAD DE BUENOS AIRES on July 5, 2012

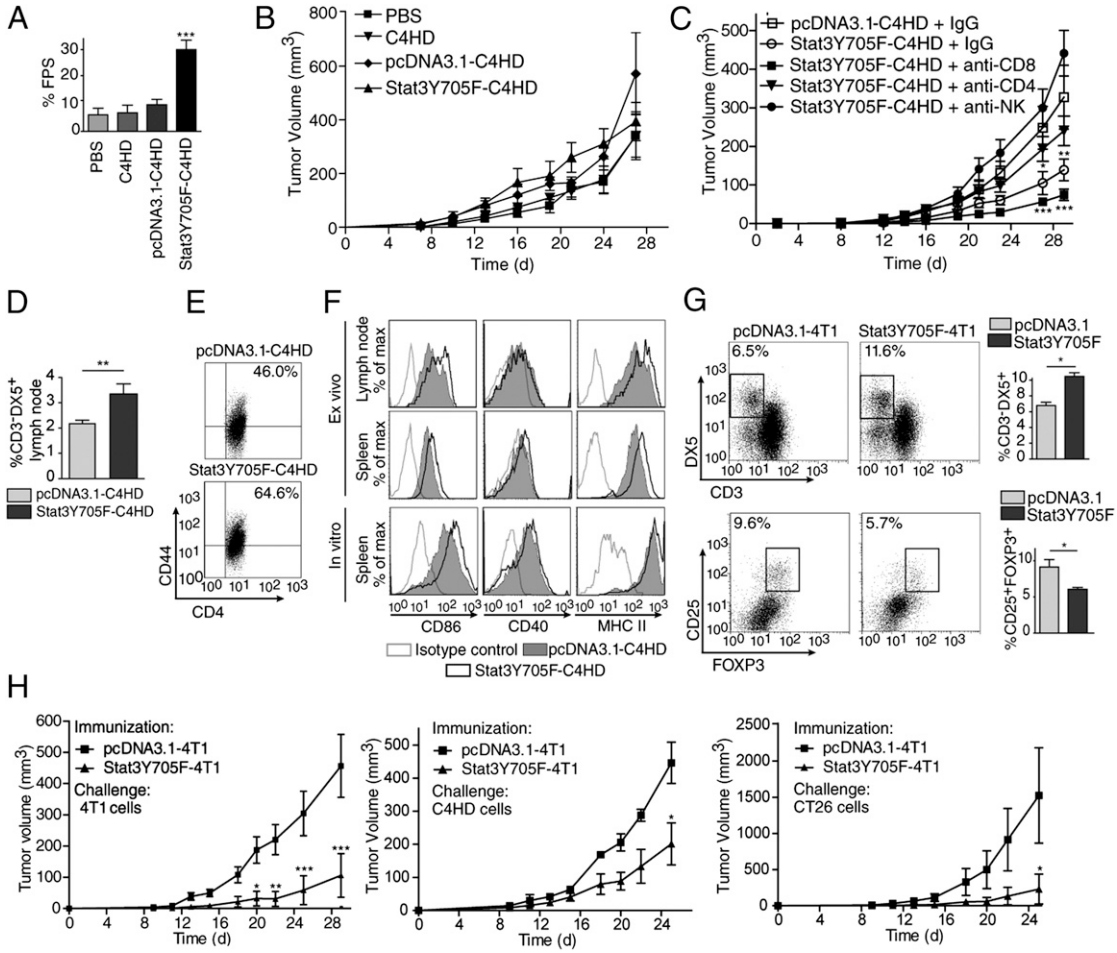

FIGURE 3. Cell-mediated immunity triggered by immunization with Stat3Y705F-breast cancer cells. (**A**) A DTH was performed in immunized BALB/c mice ($n = 5$) 1 wk after the last immunization. Data are presented as the mean ± SE of the footpad swelling index (FPS). $***p < 0.001$. (**B**) Nude mice ($n = 5$) were immunized and challenged as described in Fig. 2A. (**C**) Selective depletion of the $CD4^+$ T cell, $CD8^+$ T cell, or NK cell subsets was performed by i.p. injection of BALB/c immunized mice ($n = 5$) with mAbs specific for CD4, CD8, or NK cells as described in *Materials and Methods*. Control mice were injected with rat IgG or rabbit IgG. $*p < 0.05$, $**p < 0.01$, $***p < 0.001$ (Stat3Y705F-C4HD cells versus pcDNA3.1-C4HD cells). Similar results were obtained in two independent experiments. (**D**) NK cells were determined as $CD3^-DX5^+$ population in lymph nodes using fluorescent Abs. The fluorescence was analyzed by flow cytometry, and the percentage of NK cells of each experimental group is shown. $**p < 0.01$. (**E**) Spleen cells from mice immunized with Stat3Y705F-C4HD cells or pcDNA3.1-C4HD cells were stained with Abs specific to CD3, CD4, and CD44 and were then subjected to flow cytometry analysis to calculate the frequencies of memory T cells. Number in the upper quadrant represents the percentages of $CD3^+CD4^+CD44^+$. (**F**) Activation of DCs from spleen and lymph nodes. Ex vivo splenic and lymph node $CD11c^+$ DCs from immunized animals were analyzed for their activation status by assessing the surface expression of CD40, CD86, and MHC class II molecules by flow cytometry. Splenic DCs from immunized mice were analyzed for in vitro stimulation after coculture with mitomycin C-treated C4HD cells. (**G**) Tumor-infiltrating lymphocytes from 4T1-transfected cells immunized animals (Fig. 2C) were analyzed by flow cytometry. The percentage of NK cells ($CD3^-DX5^+$) among total leukocytes and the frequency of Tregs ($CD4^+CD25^+Foxp3^+$) among $CD4^+$ T lymphocytes in tumors from mice immunized with Stat3Y705F-4T1–transfected or pcDNA3.1-transfected cells are shown (numbers in the upper left quadrants and upper right quadrants, respectively). Percentage of NK cells and Tregs of each experimental group is shown. $*p < 0.05$ ($n = 5$). (**H**) Immunization with Stat3Y70F-4T1 cells provides cross-protection to C4HD and CT26 tumor challenge. BALB/c mice were immunized with 4T1 cells transfected with Stat3Y705F or pcDNA3.1 as described previously. Mice were then challenged with 10^4 4T1 cells (*left panel*), a fragment of C4HD tumor and injected with a depot–MPA (*center panel*), or with 4×10^5 CT26 cells (*right panel*). Each point represents the mean volume ± SE of five independent tumors. Similar results were obtained in two experiments. $*p < 0.05$, $**p < 0.01$, $***p < 0.001$.

increase in the number of tumor-infiltrating NK cells and a decrease in tumor-infiltrating T regulatory lymphocytes (Tregs) ($CD4^+CD25^+Foxp3^+$) when compared with pcDNA3.1-4T1–immunized mice (Fig. 3G). Taken together, these results indicate that vaccination with Stat3Y705F-transfected breast cancer cells leads to NK cell tumor infiltration and that both NK cells and $CD4^+$ T cells are necessary to elicit the antitumor effect observed following immunization. Moreover, MHC class II and CD86 upregulation in DCs and increase in the $CD4^+$ T memory cells, suggest that immunization with Stat3Y705F-transfected breast cancer cells promotes DCs maturation and retains the antitumor effect through $CD4^+$ T memory cell population.

To evaluate whether the protective antitumor activity following Stat3Y705F-breast cancer cell immunization was specific, we challenged mice immunized with Stat3Y705F-4T1 cells with C4HD cells, or with CT26 murine colon carcinoma cells, which are non-organ–related tumor cells. Interestingly, we observed that Stat3Y705F-4T1 cells immunization protected mice from the development of C4HD and CT26 tumors. This was reflected by a striking inhibition in tumor growth when compared with pcDNA3.1-4T1 cell-immunized animals (Fig. 3H). These results suggest that the immune memory developed by mice immunized with Stat3Y705F-4T1 cells induced cross-protection against other syngeneic breast tumor cells and against non-organ–related tumor cells.

Downloaded from http://jimmunol.org/ at UNIVERSIDAD DE BUENOS AIRES on July 5, 2012

Increased proliferation and cytokine production in splenocytes from Stat3Y705F-C4HD cell-immunized mice

To further investigate these in vivo findings, we performed several in vitro assays. We first assessed the capacity of splenocytes from immunized mice to proliferate in response to C4HD wild-type cells. Splenocytes from mice injected with Stat3Y705F-C4HD cells proliferated strongly in response to mitomycin C-treated C4HD cells. In contrast, splenocytes from pcDNA3.1-C4HD cells remained unresponsive (Fig. 4A). There were no differences between the total number of $CD4^+$ T cells and NK cells in the spleens of both experimental groups (data not shown). Using similar culture conditions, we assessed cytokine production by splenocytes after 48 h of coculture with C4HD cells. Splenocytes from mice immunized with Stat3Y705F-C4HD cells secreted higher levels of IFN-γ, IL-2, and IL-4 than splenocytes from mice immunized with pcDNA3.1-C4HD cells, whereas IL-10 levels were not altered (Fig. 4B). We next determined the lymphocyte population responsible for Stat3Y705F-C4HD cell immunization-induced IFN-γ production. Intracellular staining of IFN-γ showed that only Stat3Y705F-C4HD–immunized mice displayed an increase in the number of IFN-γ–producing $CD4^+$ T cells and NK cells upon activation of splenocytes by C4HD cells (Fig. 4C, 4D). Stimulation of splenocytes derived from animals immunized with Stat3Y705F-C4HD cells with IL-12 resulted in a higher percentage of IFN-γ–secreting NK cells than that observed upon stimulation of cells from pcDNA3.1-C4HD cell-immunized mice (Fig. 4D). We did not detect any changes in either basal or C4HD-induced IFN-γ production in $CD3^+CD8^+$ T cells (data not shown). To determine whether tumor-infiltrating NK cells and $CD4^+$ T cells from mice immunized with Stat3Y705F-4T1 cells were also able to produce more IFN-γ and to become more activated than that from pcDNA3.1-4T1–immunized mice, we evaluated the expression of this cytokine and CD69 activation marker in both cell populations. We observed an augment of the number of NK cell- and $CD4^+$ T cell-producing IFN-γ (Fig. 4E). In agreement with this result, CD69 expression was upregulated in NK cells and $CD4^+$ T cells from mice immunized with Stat3Y705F-4T1 cells versus cells from pcDNA3.1-4T1–immunized mice (Fig. 4E). These findings reveal that IFN-γ secretion in Stat3Y705F-breast cancer cell-immunized animals depends on $CD4^+$ T cells and NK cells that reside in spleen and in tumor milieu.

NK cells are responsible for the antitumor cytotoxicity induced by immunization with Stat3Y705F-C4HD cells

To evaluate the cytotoxic potential of splenocytes from mice immunized with Stat3Y705F-C4HD cells, we cocultured splenocytes from the experimental groups for 5 d in the presence of mitomycin C-treated C4HD cells. We then performed a [^{51}Cr] release assay using

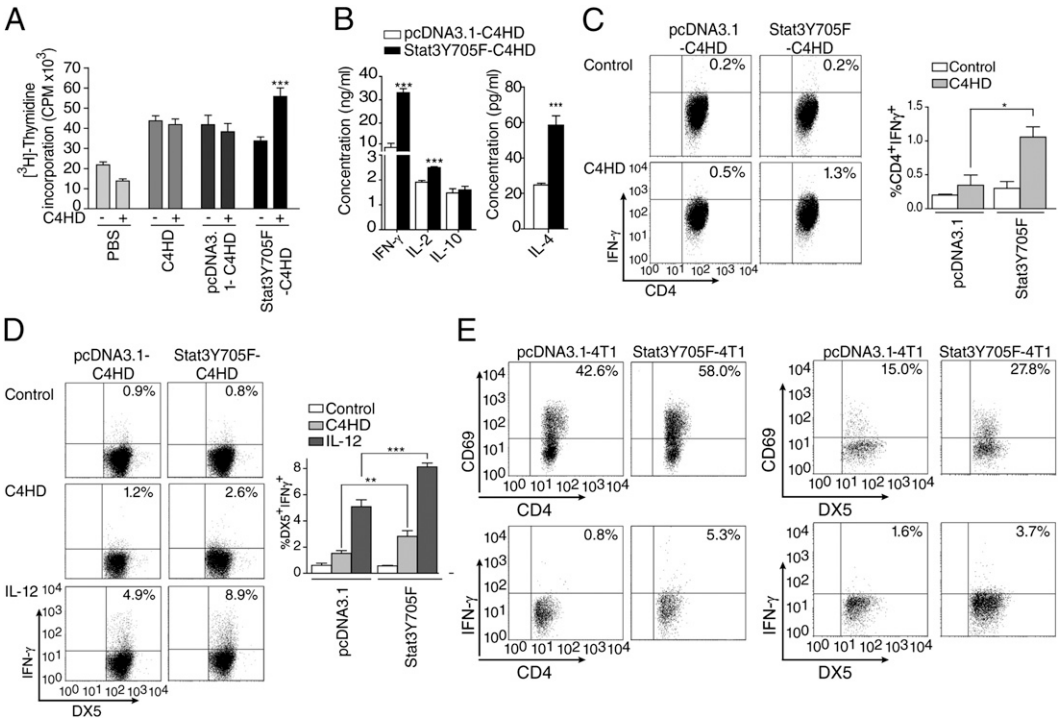

FIGURE 4. Splenocyte proliferation and cytokine secretion induced by immunization with Stat3Y705F-C4HD cells. (**A**) BALB/c mice were immunized as described in Fig. 2A, and 2 wk after the last injection, splenocytes were isolated and cultured at a density of 2×10^6/ml for 5 d in the presence (+) or absence (−) of 4×10^4 mitomycin C-treated C4HD cells/ml. During the last 16 h of culture, cells were pulsed with 0.5 μCi [^{3}H]thymidine. Cells were then harvested, and the incorporation of [^{3}H]thymidine was used as a measure of DNA synthesis. Data are presented as mean ± SE. ***$p < 0.001$. (**B**) Splenocytes obtained from immunized mice ($n = 5$) were cocultured with mitomycin C-treated C4HD cells for 48 h. The supernatants were evaluated for the presence of IFN-γ, IL-2, IL-10, and IL-4. ***$p < 0.001$. The results presented were obtained in a single experiment and are representative of two independent experiments. (**C** and **D**) Flow cytometry analysis of intracellular IFN-γ production by $CD4^+$ T cells and NK cells. Splenocytes from immunized mice were incubated for 18 h in the presence or absence of C4HD cells. Graph bar shows mean percentage of IFN-γ–producing cells from five mice. *$p < 0.05$. (C) Cells were stained with Abs specific for CD4, CD3, and IFN-γ. Numbers in the upper right quadrants represent the percentage of $CD3^+CD4^+$ cells positive for IFN-γ. (D) NK cells were also stimulated with IL-12. Cells were stained with anti-CD3, -DX5, and –IFN-γ. Percentage of NK cells ($CD3^-DX5^+$) positive for IFN-γ is shown in the upper right quadrant. (C and D) Graph bar represents shows mean percentage of IFN-γ–producing cells from five mice. **$p < 0.01$, ***$p < 0.001$. (**E**) Tumor-infiltrating lymphocytes from 4T1-transfected cells immunized animals (Fig. 2C) were stimulated ex vivo with 10 ng/ml PMA and incubated with monensin for 5 h. IFN-γ and CD69 expression were analyzed in $CD3^+CD4^+$ and in $CD3^+DX5^+$ cells by flow cytometry. Data shown were obtained from a pool of five mice.

Downloaded from http://jimmunol.org/ at UNIVERSIDAD DE BUENOS AIRES on July 5, 2012

C4HD cells as targets. Fig. 5A shows that splenocytes from Stat3Y705F-C4HD cell-immunized animals displayed a much higher cytotoxicity than those from the control animals. To identify the cell subset(s) responsible for the cytotoxic effect, we depleted the $CD4^+$ T cell, $CD8^+$ T cell, or NK cell populations from mouse splenocytes by immunomagnetic separation. We observed that only NK cell depletion abolished the cytotoxic activity of splenocytes from mice immunized with Stat3Y705F-C4HD cells (Fig. 5B). Moreover, enrichment of NK cells after 5 d of splenocyte-C4HD cell coculture by immunomagnetic negative selection demonstrated that NK cells from Stat3Y705F-C4HD cell-immunized animals were effective at killing not only the YAC-1 target cells (Fig. 5C) but also C4HD cells (Fig. 5D). Despite these findings, we did not detect cytotoxicity against C4HD cells in freshly isolated NK cell populations (data not shown). These data suggest that NK cells acquire cytotoxic activity after $CD4^+$ T cells contact the tumor cells. Because CD107a cell surface expression predicts cytolytic activity, we further investigated the expression of this marker on NK cells. As shown in Fig. 5E, NK cells from Stat3Y705F-C4HD cell–immunized mice cultured in the presence of C4HD cells displayed higher surface expression of CD107a than NK cells from pcDNA3.1-C4HD cell-immunized mice. NK cell cytotoxicity depends on the balance between stimulatory and inhibitory receptor signaling; therefore, we next asked whether C4HD cells express ligands that induce NK cell-mediated C4HD cell lysis. Flow cytometric analysis showed positive staining for H-60 and dim staining for RAE-1, both of which are ligands for the stimulating receptor NKG2D, in C4HD cells (Supplemental Fig. 3). Stat3Y705F-C4HD or Stat3Y705F-4T1 cells show no modulation on H-60 or RAE-1 expression in comparison with pcDNA3.1-transfected counterparts (data not shown). These results strongly indicate that the cytotoxic effector function induced by immunization with Stat3Y705F-C4HD cells is restricted to NK cells and that C4HD and 4T1 cells are suitable NK cell targets.

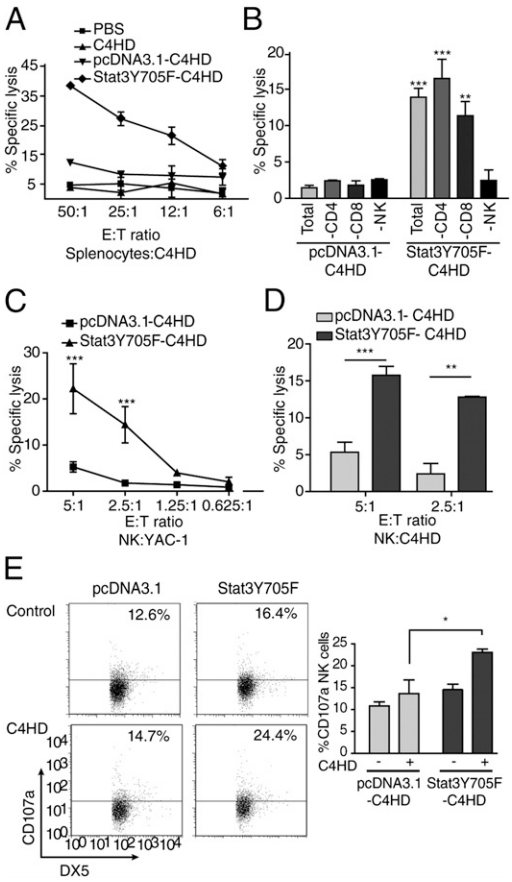

FIGURE 5. In vitro analysis of splenocyte and NK cell cytotoxicity against C4HD tumor cells. (**A**) Splenocytes obtained from immunized mice (n = 5/group) were cocultured with mitomycin C-treated C4HD cells for 5 d, and a standard chromium release assay was performed. C4HD cells were used as target cells (1×10^4 cells/well) at different E:T ratios. (**B**) Splenocytes (1×10^6 cells) were depleted of $CD4^+$ T cells, $CD8^+$ T cells, or NK cells by immunomagnetic separation or left undepleted (total) before the addition of C4HD target cells (1×10^4 cells/well) ($^{**}p < 0.01$, $^{***}p < 0.001$). (**C** and **D**) In vitro NK cell cytotoxic activity. The cytolytic activity of purified NK cells from mice immunized with Stat3Y705F-C4HD or pcDNA3.1-C4HD cells against the NK cell-sensitive target cell line YAC-1 (C) or C4HD cells (D) was tested in a standard 4-h chromium release assay. NK cells were isolated by immunomagnetic separation using negative selection. $^{**}p < 0.01$, $^{***}p < 0.001$. (**E**) Degranulation of NK cells triggered by C4HD cells. Splenocytes from immunized mice were cultured alone or with mitomycin C-treated C4HD cells, and the expression of CD107a was evaluated in the NK cell population ($CD3^-DX5^+$). Percentage of NK cells positive for CD107a of each experimental group is shown. Results correspond to one of three independent experiments (data are expressed as mean ± SE). $^*p < 0.05$.

Immunization with Stat3Y705F-breast cancer cells is effective in therapeutic administration

The strong inhibition of tumor growth observed after immunization with Stat3Y705F-Stat3 C4HD cells prompted us to study whether this protocol could be applied in a therapeutic manner mirroring the clinical situation in patients with cancer. We challenged mice with C4HD tumors in the presence of depot–MPA, and when tumors were palpable (25 mm^3) on day 6, the animals were injected with irradiated Stat3Y705F-transfected C4HD cells or with pcDNA3.1-transfected C4HD cells. The injections were repeated on day 18. Immunization with Stat3Y705F-C4HD cells inhibited tumor growth (Fig. 6A, Table II) and resulted in decreased tumor weight (Fig. 6B) when compared with mice injected with pcDNA3.1-C4HD cells. Histopathological analysis revealed that tumors from mice immunized with Stat3Y705F-C4HD cells showed a significantly lower histological grade (grade 2) and displayed more extensive necrotic and fibrotic areas with fewer mitotic figures per field than did tumors from animals injected with pcDNA3.1-C4HD cells. These tumors showed a histological grade of 3 and displayed an elevated number of mitotic figures (Supplemental Fig. 4A). We also examined whether immunization with Stat3Y705F-C4HD cells could recruit lymphocytes within the tumor microenvironment. Flow cytometric analysis of tumor-infiltrating lymphocytes showed an increase in NK cells when compared with pcDNA3.1-C4HD cell-immunized mice. $CD4^+$ T cell infiltration was evident in many but not in all mice, whereas $CD8^+$ T cells remained unchanged (Supplemental Fig. 4B).

We next challenged BALB/c mice with 4T1 cells on day 0, and when tumors were palpable (20 mm^3) on day 4, we immunized them with irradiated Stat3Y705F-4T1 or pcDNA3.1-4T1 cells. The immunizations were repeated on days 11 and 18. On day 35, we observed significant inhibition of tumor growth (Fig. 6C) and decreased tumor weight (Fig. 6D) in Stat3Y705F-4T1 cell-immunized animals when compared with mice immunized with pcDNA3.1-4T1 cells ($p < 0.05$; Table II). A decrease in metastasis was also observed ($p < 0.05$; Fig. 6E). Histopathological studies of tumors from mice immunized with Stat3Y705F-4T1 cells showed a significantly lower histological grade, with a decrease in anisokaryosis and fewer mitotic figures per field than the observed in tumors from animals injected with pcDNA3.1-4T1 cells (data not shown). These findings demonstrate for the first time, to our knowledge, that Stat3Y705F-breast cancer cell immunization is effective, even in the presence of an established primary tumor, suggesting the therapeutic potential of this cancer cell immunization protocol.

Downloaded from http://jimmunol.org/ at UNIVERSIDAD DE BUENOS AIRES on July 5, 2012

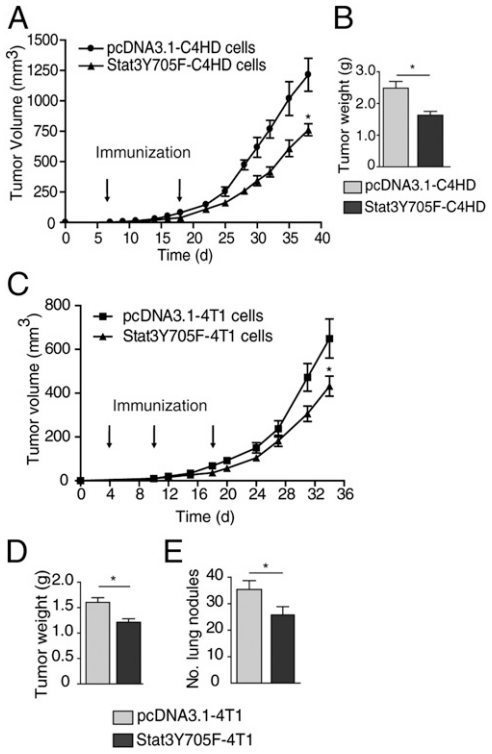

FIGURE 6. Induction of an antitumor immune response after therapeutic administration of Stat3Y705F-breast cancer cells. (**A**) On day 0, BALB/c mice ($n = 5$) were inoculated s.c. with C4HD wild-type tumor cells and implanted with depot–MPA. The mice were then treated with 2×10^6 irradiated C4HD-Stat3Y705F cells or pcDNA3.1-C4HD cells on days 6 and 18. $*p < 0.05$, mice immunized with Stat3Y705F-C4HD cells versus control mice. Similar results were obtained in three independent experiments. (**B**) Final tumor weight of mice immunized with Stat3Y705F-C4HD cells or pcDNA3.1-C4HD cells. (**C**) On day 0, BALB/c mice ($n = 8$) were inoculated with 1×10^4 4T1 cells. The mice were then treated with 1×10^6 irradiated Stat3Y705F-4T1 cells or pcDNA3.1-4T1 cells on days 4, 11, and 18. The mice were assessed for the formation of tumors three times a week. (**D**) Final tumor weights of mice immunized with Stat3Y705F-4T1 cells or pcDNA3.1-4T1 cells. (**E**) The immunized mice were sacrificed, lungs were harvested and fixed, and the number of 4T1 tumor nodules was counted. Values represent means ± SE ($n = 8$). Similar results were obtained in three independent experiments. $*p < 0.05$.

Discussion

Our findings demonstrate that inhibition of Stat3 activation in tumor cells results in a shift from a tumor-enhancing phenotype to an inflammatory antitumor phenotype that can be successfully applied as an immunotherapy against breast cancer in either a prophylactic or a therapeutic manner. Our studies in primary breast cancer C4HD cells, in which Stat3 activation is induced by MPA, and in 4T1 cells, which display constitutive activation of Stat3, show that immunization with DN Stat3-transfected cells results in inhibition of tumor growth and prevention of metastasis. Moreover, we demonstrated that mice immunized with DN Stat3-4T1 cells developed an antitumor immune response that provided cross-protection against other sygenenic breast cancer, such as C4HD, cells and against CT26 colon carcinoma cells. Furthermore, we have demonstrated for the first time, to our knowledge, that similar to the effects of MYC inactivation (11), Stat3 inactivation results in cellular senescence.

Stat3 activation is tightly controlled in normal cells, because preventing its hyperactivation is necessary to maintain immune homeostasis. In contrast, Stat3 is constitutively active in cancer cells, resulting in dampened immune responses and leading to tumor evasion. In accord with previous reports on melanoma, colon carcinoma, sarcoma, and diffuse large B cell lymphoma cell lines (6, 26, 27), our results show that blocking Stat3 signaling in breast cancer cells, by transfection with the Stat3Y705F vector or by treatment with the pharmacological inhibitor JSI-124, induces upregulation of the proinflammatory cytokines TNF-α, IFN-γ, IL-6, and IL-5, as well as chemokines, including IP-10 and RANTES. Thus, transfection with a DN Stat3 vector results in a tumor cell that potentially has the ability to neutralize immunosuppressive signals derived from parental tumors, creating a favorable microenvironment for immune recognition. Wang et al. (6) demonstrated that supernatant from v-Src–transformed BALB/c 3T3 fibroblasts expressing a DN Stat3 vector induced DC maturation. In addition, inhibition of Stat3 signaling in DCs by JSI-124 treatment resulted in a maturation of these cells in the presence of tumor-derived factors (28). In line with this evidence, in this work, we demonstrated that DCs from mice immunized with Stat3Y705F-C4HD cells cocultivated with C4HD cells were able to upregulate CD86 and MHC class II molecules, markers of DC maturation. Importantly, tumor cells transfected with DN Stat3 vector or treated with JSI-124 released TNF-α and IFN-γ, which can act synergistically to induce signaling in Ag-specific $CD4^+$ T cells that prevents tumor angiogenesis, tumor cell proliferation, and multistage carcinogenesis (29). In addition, these cells produced RANTES, which is involved in T cell migration and NK cell recruitment to tumors (30), and IP-10, which is a chemoattractant for resting NK cells and activated T cells (31).

Through depletion experiments, we found that the loss of $CD4^+$ T cells or NK cells but not the loss of $CD8^+$ T cells was sufficient to impede the antitumor effect of immunization with Stat3Y705F-

Table II. Therapeutic whole-cell vaccine

Protocol and Treatment	Mean Tumor Volume ± SEM (mm^3)	Mean Growth Rate ± SEM (mm^3/d)	% Growth Inhibition
C4HD immunization			
pcDNA3.1-C4HD	1025.0 ± 333.4[a]	32.4 ± 2.2[a]	
Stat3Y705F-C4HD	762.3 ± 140.1[b]	19.2 ± 1.2[b]	46.6[c]
4T1 immunization			
pcDNA3.1-4T1	522.5 ± 44.1[a]	27.3 ± 2.9[a]	
Stat3Y705F-4T1	326.6 ± 56.33[b]	18.4 ± 1.4[b]	37.5[d]

Growth rates were calculated as the slopes of growth curves. Volume and percentage of growth inhibition in tumors from mice immunized with Stat3Y705F-C4HD cells with respect to mice immunized with control pcDNA3.1-C4HD cells were calculated at day 38. Volume and percentage of growth inhibition in tumors from mice immunized with Stat3Y705F-4T1 cells with respect to mice immunized with control pcDNA3.1-4T1 cells were calculated at day 33, as described in *Materials and Methods*.

[a]versus [b], $p < 0.001$.

[c]With respect to pcDNA3.1-C4HD cells, for growth inhibition, $p < 0.001$.

[d]With respect to pcDNA3.1-4T1 cells, for growth inhibition, $p < 0.01$.

Downloaded from http://jimmunol.org/ at UNIVERSIDAD DE BUENOS AIRES on July 5, 2012

transfected cells in BALB/c mice. We further determined that only NK cells from Stat3Y705F-C4HD–immunized mice had the ability to degranulate and to lyse parental C4HD cells. We also observed a strong increase in IFN-γ secretion by splenocytes from Stat3Y705F-C4HD–immunized animals upon coculture with C4HD cells and found that $CD4^+$ T cells and NK cells were the main source of IFN-γ production. In contrast, immunization of nude mice demonstrated no significant inhibition of tumor growth. Our data also reveal the generation of $CD4^+$ memory T cells and activation of DCs along Stat3Y705F-breast cancer cell immunization. Taken as a whole, the studies presented in this work support the notion that $CD4^+$ T cells, activated by DCs, are required for the antitumor immune response elicited by immunization with Stat3Y705F-breast cancer cells and in them reside the immunological memory for tumor recognition. NK cells are the effector/cytotoxic cells that depend on $CD4^+$ T cell activation/cooperation.

NK cell cytotoxic activity is regulated by the integration of signals from inhibitory and activating receptors (32). Of particular interest is the activating receptor NKG2D, which binds to several cell surface glycoproteins in mice, including the RAE-1 proteins and the minor histocompatibility Ag H-60 (33). In this work, we showed that C4HD cells expressed RAE-1 and H-60, and previous studies have demonstrated the expression of these Ags in 4T1 cells (34), indicating that both cancer cell lines are capable of triggering NK cell cytotoxic responses, resulting in tumor clearance.

The fact that DN-breast cancer immunotherapy confers cross-protection against other breast cancers and against a different type of cancer with respect to the parental one, turns it into a potentially very attractive, more practical, and generic tumor vaccine. Different immunization strategies have achieved an immune response that provides tumor cross-protection, such as the administration of colon carcinoma CT26 cells transfected with an IL-12 plasmid, was able to reject the murine breast cancer line LM3 through the participation of CTLs (35), and immunization with irradiated defined human embryonic stem cells was effective at rejecting CT26 cells along with the induction of IFN-γ–producing $CD4^+$ T cells (36). However, in vivo NK cell participation in these works was not evaluated. Our findings hold that the antitumor effect of DN-breast cancer immunization requires not only NK cells as effectors, but also $CD4^+$ T cells, suggesting that tumor Ags shared by the different cell types might be targeted along this therapy to achieve cross-protection activity.

To our knowledge, our data provide the first demonstration that Stat3 inhibition induces a cellular senescence program. Seminal findings of Wu et al. (11) showed that inactivation of the oncogene MYC in different cancer cell types induces cellular senescence. Later studies demonstrated that $CD4^+$ T cells play a central role in tumor regression upon MYC inactivation and that the secreted cytokine profile of these cells resembles that observed upon Stat3 inactivation (12). Moreover, NK cells are suggested to function as effector cells in tumor lysis in this model. It is widely known that inhibition of Stat3 activation leads to apoptosis. In particular, we have previously demonstrated that inhibition of Stat3 signaling induces apoptosis in C4HD cells (19); however, we found that UV-irradiated apoptotic C4HD cells were not able to trigger an antitumor immune response (20). In this study, we have shown that C4HD and 4T1 cells transfected with the Stat3Y705F vector undergo senescence as determined by several characteristic molecular features, including elevated SA-β-gal activity, increased expression of the cell cycle inhibitors p15INK4b and p16INK4a, and characteristic changes in chromatin structure, such as increased histone H3 K9 methylation. Taken together, these findings demonstrate that immunization with these senescent tumor cells could contribute to the tumor phenotypic change that finally leads to an effective antitumor immune response.

Experiments using 4T1 cells as a model of metastatic breast cancer showed that immunization with Stat3Y705F-transfected 4T1 cells inhibits tumor growth and lung metastasis. Interestingly, we found a decrease in the number of Tregs and an increase in NK cells infiltrating tumors of Stat3Y705F-4T1 cell-immunized animals when compared with pcDNA-4T1 cell-immunized animals. This inverse correlation between Tregs and NK cells is supported by the findings of Olkhanud et al. (37) who demonstrated that Tregs are necessary for 4T1 lung metastasis and that protection against metastasis resides in the NK cell population.

Immunization with DN Stat3-transfected breast cancer cells also proved effective for therapeutic administration. Interestingly, tumors obtained from mice immunized with pcDNA3.1-transfected cancer cells had higher histological grades and tumor sizes than those from mice immunized with Stat3Y705F-transfected cancer cells. A 10-y follow-up of breast cancer patients showed that tumor size, nodal status, and tumor grade remained the most important prognostic factors for long-term survival (38) and were also predictors for distant metastasis (39). Importantly, we found that immunization with Stat3-inhibited breast cancer cells decreased tumor grade, tumor growth, and metastasis, the most important prognostic indicators in breast cancer.

Targeting Stat3 as a tool for cancer immunotherapy continues to be explored using multiple strategies. These approaches, which include in vivo blocking of Stat3 by using genetic deletions in tumor cells or in tumor-infiltrating immune cells or by administration of pharmacological inhibitors, have variable rates of success in stimulating antitumor immune responses (5, 27, 40, 41); however, both of these approaches have limited clinical application until target-specific delivery is possible. To our knowledge, our study provides the first report of the use of ex vivo Stat3-inactivated tumor cells as an immunotherapy; this approach has the advantage of immunizing the host with the whole array of Ags expressed by the tumor cells in a stimulatory microenvironment composed of multiple proinflammatory cytokines and chemokines to generate an antitumor immune response.

In conclusion, we demonstrated that ablating Stat3 signaling in breast cancer cells results in an effective immunogen able to activate the immune surveillance system that inhibits breast cancer growth and metastasis. To our knowledge, the induction of cellular senescence after Stat3 inactivation is a novel finding that opens new avenues for immunotherapy research and clinical application.

Acknowledgments

The authors wish to thank Dr. Alfredo A. Molinolo (National Institutes of Health, Bethesda, MD) for constant help and support.

Disclosures

The authors have no financial conflicts of interest.

References

1. Bromberg, J. F., M. H. Wrzeszczynska, G. Devgan, Y. Zhao, R. G. Pestell, C. Albanese, and J. E. Darnell, Jr. 1999. Stat3 as an oncogene. *Cell* 98: 295–303.
2. Buettner, R., L. B. Mora, and R. Jove. 2002. Activated STAT signaling in human tumors provides novel molecular targets for therapeutic intervention. *Clin. Cancer Res.* 8: 945–954.
3. Rabinovich, G. A., D. Gabrilovich, and E. M. Sotomayor. 2007. Immunosuppressive strategies that are mediated by tumor cells. *Annu. Rev. Immunol.* 25: 267–296.
4. Yu, H., M. Kortylewski, and D. Pardoll. 2007. Crosstalk between cancer and immune cells: role of STAT3 in the tumour microenvironment. *Nat. Rev. Immunol.* 7: 41–51.
5. Kortylewski, M., and H. Yu. 2008. Role of Stat3 in suppressing anti-tumor immunity. *Curr. Opin. Immunol.* 20: 228–233.

Downloaded from http://jimmunol.org/ at UNIVERSIDAD DE BUENOS AIRES on July 5, 2012

6. Wang, T., G. Niu, M. Kortylewski, L. Burdelya, K. Shain, S. Zhang, R. Bhattacharya, D. Gabrilovich, R. Heller, D. Coppola, et al. 2004. Regulation of the innate and adaptive immune responses by Stat-3 signaling in tumor cells. *Nat. Med.* 10: 48–54.
7. Bowman, T., R. Garcia, J. Turkson, and R. Jove. 2000. STATs in oncogenesis. *Oncogene* 19: 2474–2488.
8. Yu, H., and R. Jove. 2004. The STATs of cancer—new molecular targets come of age. *Nat. Rev. Cancer* 4: 97–105.
9. Gritsko, T., A. Williams, J. Turkson, S. Kaneko, T. Bowman, M. Huang, S. Nam, I. Eweis, N. Diaz, D. Sullivan, et al. 2006. Persistent activation of stat3 signaling induces survivin gene expression and confers resistance to apoptosis in human breast cancer cells. *Clin. Cancer Res.* 12: 11–19.
10. Real, P. J., A. Sierra, A. De Juan, J. C. Segovia, J. M. Lopez-Vega, and J. L. Fernandez-Luna. 2002. Resistance to chemotherapy via Stat3-dependent overexpression of Bcl-2 in metastatic breast cancer cells. *Oncogene* 21: 7611–7618.
11. Wu, C. H., J. van Riggelen, A. Yetil, A. C. Fan, P. Bachireddy, and D. W. Felsher. 2007. Cellular senescence is an important mechanism of tumor regression upon c-Myc inactivation. *Proc. Natl. Acad. Sci. USA* 104: 13028–13033.
12. Rakhra, K., P. Bachireddy, T. Zabuawala, R. Zeiser, L. Xu, A. Kopelman, A. C. Fan, Q. Yang, L. Braunstein, E. Crosby, et al. 2010. $CD4^+$ T cells contribute to the remodeling of the microenvironment required for sustained tumor regression upon oncogene inactivation. *Cancer Cell* 18: 485–498.
13. Rivas, M. A., R. P. Carnevale, C. J. Proietti, C. Rosemblit, W. Beguelin, M. Salatino, E. H. Charreau, I. Frahm, S. Sapia, P. Brouckaert, et al. 2008. TNFα acting on TNFR1 promotes breast cancer growth via p42/P44 MAPK, JNK, Akt and NF-κB–dependent pathways. *Exp. Cell Res.* 314: 509–529.
14. Institute of Laboratory Animal Resources, Commission on Life Sciences, National Research Council. 1996. *Guide for the Care and Use of Laboratory Animals.* National Academy Press, Washington, DC.
15. Lanari, C., C. A. Lamb, V. T. Fabris, L. A. Helguero, R. Soldati, M. C. Bottino, S. Giulianelli, J. P. Cerliani, V. Wargon, and A. Molinolo. 2009. The MPA mouse breast cancer model: evidence for a role of progesterone receptors in breast cancer. *Endocr. Relat. Cancer* 16: 333–350.
16. Salatino, M., R. Schillaci, C. J. Proietti, R. Carnevale, I. Frahm, A. A. Molinolo, A. Iribarren, E. H. Charreau, and P. V. Elizalde. 2004. Inhibition of in vivo breast cancer growth by antisense oligodeoxynucleotides to type I insulin-like growth factor receptor mRNA involves inactivation of ErbBs, PI-3K/Akt and p42/p44 MAPK signaling pathways but not modulation of progesterone receptor activity. *Oncogene* 23: 5161–5174.
17. Rivas, M. A., M. Tkach, W. Beguelin, C. J. Proietti, C. Rosemblit, E. H. Charreau, P. V. Elizalde, and R. Schillaci. 2010. Transactivation of ErbB-2 induced by tumor necrosis factor α promotes NF-κB activation and breast cancer cell proliferation. *Breast Cancer Res. Treat.* 122: 111–124.
18. Bromberg, J. F., C. M. Horvath, D. Besser, W. W. Lathem, and J. E. Darnell, Jr. 1998. Stat3 activation is required for cellular transformation by v-src. *Mol. Cell. Biol.* 18: 2553–2558.
19. Proietti, C., M. Salatino, C. Rosemblit, R. Carnevale, A. Pecci, A. R. Kornblihtt, A. A. Molinolo, I. Frahm, E. H. Charreau, R. Schillaci, and P. V. Elizalde. 2005. Progestins induce transcriptional activation of signal transducer and activator of transcription 3 (Stat3) via a Jak- and Src-dependent mechanism in breast cancer cells. *Mol. Cell. Biol.* 25: 4826–4840.
20. Schillaci, R., M. Salatino, J. Cassataro, C. J. Proietti, G. H. Giambartolomei, M. A. Rivas, R. P. Carnevale, E. H. Charreau, and P. V. Elizalde. 2006. Immunization with murine breast cancer cells treated with antisense oligodeoxynucleotides to type I insulin-like growth factor receptor induced an antitumoral effect mediated by a $CD8^+$ response involving Fas/Fas ligand cytotoxic pathway. *J. Immunol.* 176: 3426–3437.
21. Dimri, G. P., X. Lee, G. Basile, M. Acosta, G. Scott, C. Roskelley, E. E. Medrano, M. Linskens, I. Rubelj, O. Pereira-Smith, et al. 1995. A biomarker that identifies senescent human cells in culture and in aging skin in vivo. *Proc. Natl. Acad. Sci. USA* 92: 9363–9367.
22. Dexter, D. L., H. M. Kowalski, B. A. Blazar, Z. Fligiel, R. Vogel, and G. H. Heppner. 1978. Heterogeneity of tumor cells from a single mouse mammary tumor. *Cancer Res.* 38: 3174–3181.
23. Aslakson, C. J., and F. R. Miller. 1992. Selective events in the metastatic process defined by analysis of the sequential dissemination of subpopulations of a mouse mammary tumor. *Cancer Res.* 52: 1399–1405.
24. Ling, X., and R. B. Arlinghaus. 2005. Knockdown of STAT3 expression by RNA interference inhibits the induction of breast tumors in immunocompetent mice. *Cancer Res.* 65: 2532–2536.
25. Blaskovich, M. A., J. Sun, A. Cantor, J. Turkson, R. Jove, and S. M. Sebti. 2003. Discovery of JSI-124 (cucurbitacin I), a selective Janus kinase/signal transducer and activator of transcription 3 signaling pathway inhibitor with potent antitumor activity against human and murine cancer cells in mice. *Cancer Res.* 63: 1270–1279.
26. Burdelya, L., M. Kujawski, G. Niu, B. Zhong, T. Wang, S. Zhang, M. Kortylewski, K. Shain, H. Kay, J. Djeu, et al. 2005. Stat3 activity in melanoma cells affects migration of immune effector cells and nitric oxide-mediated antitumor effects. *J. Immunol.* 174: 3925–3931.
27. Scuto, A., M. Kujawski, C. Kowolik, L. Krymskaya, L. Wang, L. M. Weiss, D. Digiusto, H. Yu, S. Forman, and R. Jove. 2011. STAT3 inhibition is a therapeutic strategy for ABC-like diffuse large B-cell lymphoma. *Cancer Res.* 71: 3182–3188.
28. Nefedova, Y., P. Cheng, D. Gilkes, M. Blaskovich, A. A. Beg, S. M. Sebti, and D. I. Gabrilovich. 2005. Activation of dendritic cells via inhibition of Jak2/STAT3 signaling. *J. Immunol.* 175: 4338–4346.
29. Müller-Hermelink, N., H. Braumüller, B. Pichler, T. Wieder, R. Mailhammer, K. Schaak, K. Ghoreschi, A. Yazdi, R. Haubner, C. A. Sander, et al. 2008. TNFR1 signaling and IFN-γ signaling determine whether T cells induce tumor dormancy or promote multistage carcinogenesis. *Cancer Cell* 13: 507–518.
30. Wendel, M., I. E. Galani, E. Suri-Payer, and A. Cerwenka. 2008. Natural killer cell accumulation in tumors is dependent on IFN-γ and CXCR3 ligands. *Cancer Res.* 68: 8437–8445.
31. Arenberg, D. A., S. L. Kunkel, P. J. Polverini, S. B. Morris, M. D. Burdick, M. C. Glass, D. T. Taub, M. D. Iannettoni, R. I. Whyte, and R. M. Strieter. 1996. Interferon-γ–inducible protein 10 (IP-10) is an angiostatic factor that inhibits human non-small cell lung cancer (NSCLC) tumorigenesis and spontaneous metastases. *J. Exp. Med.* 184: 981–992.
32. Pegram, H. J., D. M. Andrews, M. J. Smyth, P. K. Darcy, and M. H. Kershaw. 2011. Activating and inhibitory receptors of natural killer cells. *Immunol. Cell Biol.* 89: 216–224.
33. Diefenbach, A., A. M. Jamieson, S. D. Liu, N. Shastri, and D. H. Raulet. 2000. Ligands for the murine NKG2D receptor: expression by tumor cells and activation of NK cells and macrophages. *Nat. Immunol.* 1: 119–126.
34. Takaki, R., Y. Hayakawa, A. Nelson, P. V. Sivakumar, S. Hughes, M. J. Smyth, and L. L. Lanier. 2005. IL-21 enhances tumor rejection through a NKG2D-dependent mechanism. *J. Immunol.* 175: 2167–2173.
35. Adris, S., E. Chuluyan, A. Bravo, M. Berenstein, S. Klein, M. Jasnis, C. Carbone, Y. Chernajovsky, and O. L. Podhajcer. 2000. Mice vaccination with interleukin 12-transduced colon cancer cells potentiates rejection of syngeneic non-organ-related tumor cells. *Cancer Res.* 60: 6696–6703.
36. Li, Y., H. Zeng, R. H. Xu, B. Liu, and Z. Li. 2009. Vaccination with human pluripotent stem cells generates a broad spectrum of immunological and clinical responses against colon cancer. *Stem Cells* 27: 3103–3111.
37. Olkhanud, P. B., D. Baatar, M. Bodogai, F. Hakim, R. Gress, R. L. Anderson, J. Deng, M. Xu, S. Briest, and A. Biragyn. 2009. Breast cancer lung metastasis requires expression of chemokine receptor CCR4 and regulatory T cells. *Cancer Res.* 69: 5996–6004.
38. Soerjomataram, I., M. W. Louwman, J. G. Ribot, J. A. Roukema, and J. W. Coebergh. 2008. An overview of prognostic factors for long-term survivors of breast cancer. *Breast Cancer Res. Treat.* 107: 309–330.
39. Rabbani, S. A., and A. P. Mazar. 2007. Evaluating distant metastases in breast cancer: from biology to outcomes. *Cancer Metastasis Rev.* 26: 663–674.
40. Kortylewski, M., M. Kujawski, T. Wang, S. Wei, S. Zhang, S. Pilon-Thomas, G. Niu, H. Kay, J. Mulé, W. G. Kerr, et al. 2005. Inhibiting Stat3 signaling in the hematopoietic system elicits multicomponent antitumor immunity. *Nat. Med.* 11: 1314–1321.
41. Liu, L., S. Nam, Y. Tian, F. Yang, J. Wu, Y. Wang, A. Scuto, P. Polychronopoulos, P. Magiatis, L. Skaltsounis, et al. 2011. 6-Bromoindirubin-3′-oxime inhibits JAK/STAT3 signaling and induces apoptosis of human melanoma cells. *Cancer Res.* 71: 3972–3979.

Downloaded from http://jimmunol.org/ at UNIVERSIDAD DE BUENOS AIRES on July 5, 2012